World Scientific
www.worldscientific.com

INSULATOR TO METAL TRANSITION AND OPTICAL RESPONSE OF CsCl UNDER PRESSURE

NAEEMULLAH[*], G. MURTAZA[†,**], R. KHENATA[‡,§],
A. H. RESHAK[¶,∥], S. NAEEM[†] and M. N. KHALID[†]

[*]Department of Physics G. D. C. Darra Adam Khel,
F. R. Kohat, KPK, Pakistan
[†]Materials Modeling Lab, Department of Physics,
Islamia College University, Peshawar
[‡]LPQ3M Laboratory, Institute of Science and Technology,
University of Mascara, Algeria
[§]Depatment of Physics and Astronomy, King Saud University,
P. O. Box 2455, Riyadh 11451, Saudi Arabia
[¶]New Technologies-Research Center, University of West Bohemia,
Univerzitni 8, 306 14 Pilsen, Czech Republic
[∥]Center of Excellence Geopolymer and Green Technology,
School of Material Engineering,
University Malaysia Perlis, 01007 Kangar, Perlis, Malaysia
[**]murtaza@icp.edu.pk

First principle calculations on cesium chloride (CsCl) compound have been performed using state of the art full potential linearized augmented plane wave (FP-LAPW) method. Calculated structural parameters are found in excellent agreement to the experimental results. Band gap of the compound decreases with the increase of pressure. At 507 GPa, electronic nature of the compound changed from the insulating to metallic. Changes are reported in the optical properties like real and imaginary parts of dielectric function, optical conductivity and reflectivity of CsCl on application of high pressure.

1. Introduction

Cesium halides binary solids have been attracting the keen interest of the scientific community because of their wide and diverse physical properties. At low temper-

---

[**]Corresponding author.

ature, cesium halides have large specific heat, nonmagnetic nature, high thermal conductivities and are nonconductor of electricity. These compounds are used in the field of nuclear medicine, cancer (brachytherapy) treatment and in the diagnosis of myocardial infarction.[1–5] They are also used in photo-cathodes at high ultraviolet wavelengths[6] and as beam-splitter in optics in wide band spectrophotometer.[7] Color centers in single crystal cesium halides, in simple cubic structure were studied by Avakian and Smakula.[8]

Cesium chloride (CsCl) is an inorganic compound adopting the cubic crystal structure with eightfold coordination. Typical unit cell contains eight ions of chlorine (Cl^-) at the corners of the cube and one cesium ion (Cs^+) at the center of the cube. The high quality CsCl single crystal has a wide transparency, ranging from ultraviolet to infrared region and therefore had been used for the cuvettes, prisms and windows in the optical spectrometers.[9] When heated to above 450°C, this compound undergoes a structural phase transition from CsCl to NaCl phase.[10] It is a wide band gap insulator of 8.35 eV at 80 K and 8.4 eV at 5 K.[11] Due to solubility of CsCl in its thin film state, Yoshikawa *et al.*[12] did some limited amount of *in situ* characterization. Tsuchiya *et al.*[13] have used its thin films as steam etchable resists in IC fabrication. The cohesive energetic of solid CsCl is studied by Pyper.[14] The infrared spectra of CsCl aqueous solutions are studied by Max and Chapados.[15] High pressure phonon study of CsCl is carried out by Nardelli *et al.*[16] Metallization under the application of pressure has been determined for some of the cesium halides e.g., the cesium iodide, with the smallest band gap and soft one of all the cesium halides is a best candidate for the band overlap metallization, which was found to be 110 GPa.[17] Eremets *et al.*[18] used direct electrical transport measurements in a diamond anvil cell and found that CsI becomes metal at 115 GPa. Vohra *et al.*[19] uses the X-ray diffraction method and report the band overlap metallization of CsI among the family of cesium halides.

In this paper, the density functional calculations are performed to investigate the structural, electronic and optical properties of CsCl in its B2 phase under the application of high pressure.

2. Computational Details

We have performed calculations using all-electrons full potential linearized augmented plane with the mixed basis full-potential linearized augumented plane wave plus local orbits (FP-LAPW + lo) method[20,21] as implemented in WIEN2K computer package.[22] Wu-Cohen generalized gradient approximation (GGA)[23] and the modified Becke–Johnson (mBJ) potential[24] are applied to treat the exchange correlation effects. The parameters for secular matrix determination is $R_{MT} * K_{max} = 7$ (R_{MT} is the Muffin-Tin sphere radii and Kmax is the cut-off wave vector in the 1st Brillouin Zone. The Muffin-Tin radii for Cs and Cl is 2.0 a.u. The integrals over the Brillouin zone are performed up to 1000 k-points in the irreducible Brillouin zone.

3. Results and Discussions

3.1. *Structural properties*

The binary CsCl compound crystallizes in the cubic structure with space group Pm-3m (#221). The typical unit cell contains the Cl^- atoms at the corner of the cube and Cs^+ at the center of the cube. The structural parameters are calculated using volume optimization process. In this process, we studied the variations of the unit cell energy with the unit cell volume. One obtains the optimized volume corresponding to the minimum energy of unit cell called ground state energy of the unit cell as shown in Fig. 1. The lattice constant, a (Å) and bulk modulus B (GPa) were obtained at different pressures are presented along with the theoretical and experimental data in Table 1. From the table, we noted that the calculated values of the lattice constants a (Å) and bulk modulus B (GPa) at zero pressure are in close agreement to the available theoretical and experimental data. Variations in lattice constant with pressure is displayed in Fig. 2. Plot shows that lattice constant decreases with increase in pressure and hence the squeezing of the unit cell.

3.2. *Electronic properties*

The calculations of the band structure at pressure range from 0 GPa to 507 GPa with a step of 100 GPa are carried out for CsCl and are depicted in Fig. 3. The
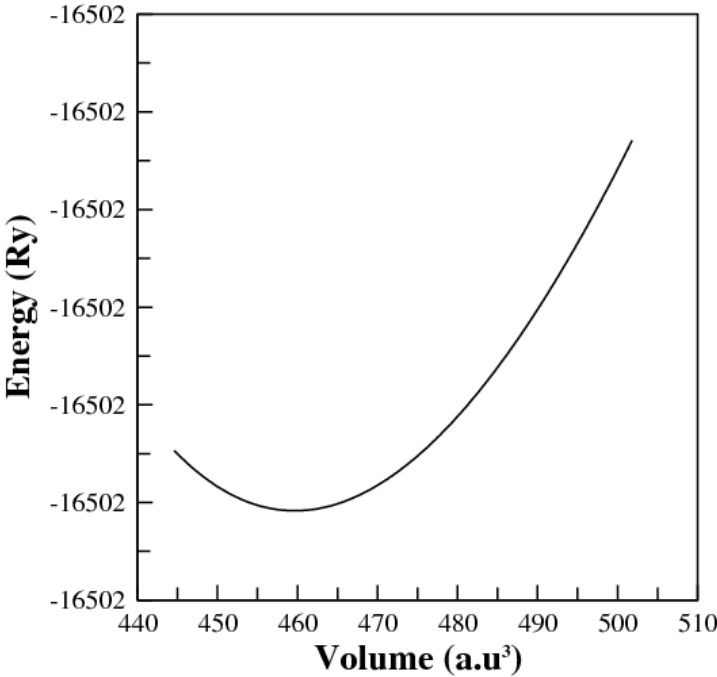

Fig. 1.   Unit cell energy as function of volume.

Table 1.   The calculated lattice constant a (Å) and bulk modulus B (GPa) along with the available experimental and theoretical values at 0 GPa.

	Lattice constant a (Å)	Bulk modulus B (GPa)
Present	4.08	17.7
Experimental	4.12[b]	22.9[c]
Theoretical	3.99[a]	24.3[a]

[a]Ref. 16
[b]Ref. 30
[c]Ref. 31
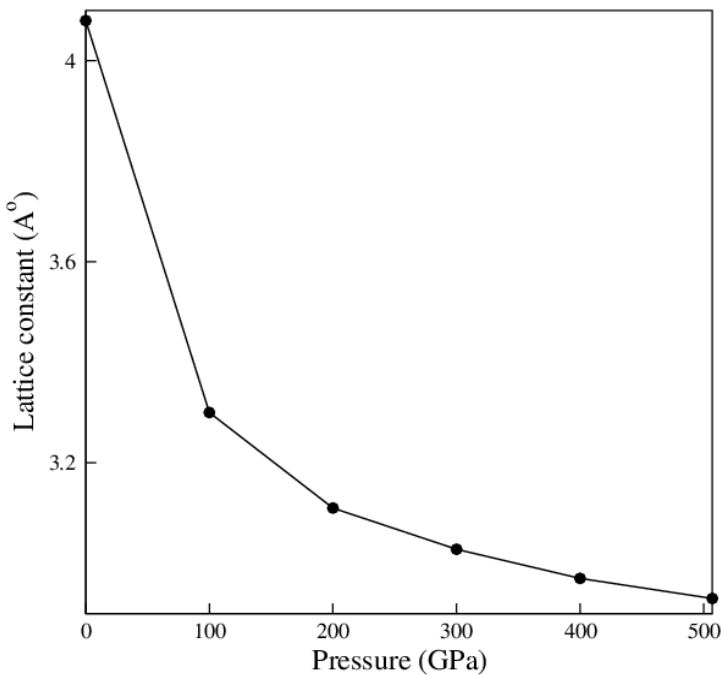
Fig. 2.   Lattice constant (Å) as a function of pressure (GPa).

calculated band gaps at different pressures are also presented in Table 2. The calculated band gap at zero pressure is 6.95 eV. This gap lies between the top of valence band and the bottom of conduction band (CB) at the Γ-symmetry point of the Brillouin zone which shows that the material is wide direct band gap insulator. At 400 GPa, the valence and conduction bands seems to be overlapping. However, the difference between the experimental band gap (8.35 eV) and calculated one at 0 GPa is 1.4 eV which is typical of density functional band gap under estimation. To remove the discrepancy and correctly determine the metallization pressure, we draw smooth curve for band gap variation with respect to pressure,
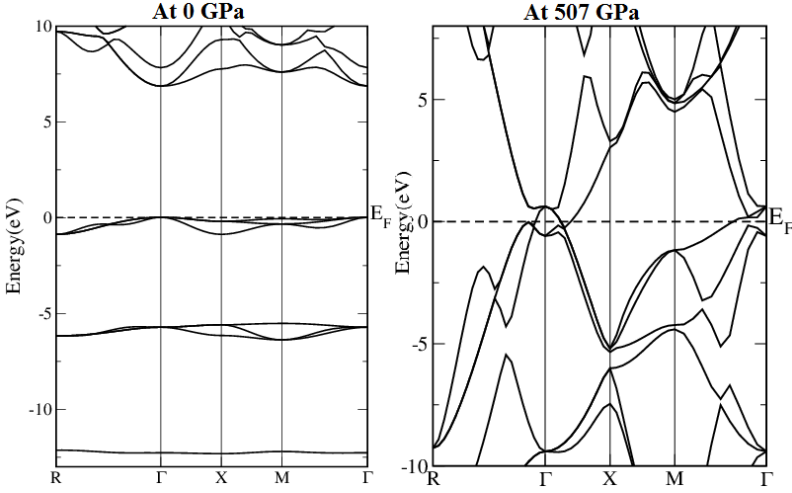
Fig. 3.   Band structure of CsCl at 0 GPa and 507 GPa.

Table 2.   Calculated band gap (eV) at different pressures (GPa).

Pressure (GPa)	Band gap (eV)	Experimental
0	6.96	8.35[a] at 80 K and 8.4[a] at 5 K
100	3.05	
200	1.4	
300	0.4	
400	metallic	
507	metallic	

[a]Ref. 11

according to Eq. (1);

$$E_g = -1.375 \times 10^{-7} p^3 + 1.371 \times 10^{-4} p^2 - 0.05023 p + 8.35 \,, \tag{1}$$

where p denotes the pressure. It is clear from this table and from Fig. 3 that the increase in pressure, encounters the decrease in band gap. At 507 GPa, the valence and conduction bands overlap (Fig. 3), therefore the electronic nature of the compound changes from insulator to metal. It is further seen that the valence band width in the absence of pressure is very small. Interestingly with the increase in pressure, the valence band width increases and is widest at 507 GPa as shown from Fig. 3. Variation in the band gap as a function of pressure is depicted in Fig. 4 using the fit equation (1).

The band structure of the compound can be further explained by the density of states (DOS). The DOS plots for 0 GPa and 507 GPa are shown in Fig. 5. The DOS plot for CsCl at 0 GPa shows that below the Fermi level, the valence band is formed by the Cl-3p state with little contribution from Cs-5p state. Three bands are seen below the valence band which are composed of Cs-5p, Cl-3s and Cs-6s, respectively
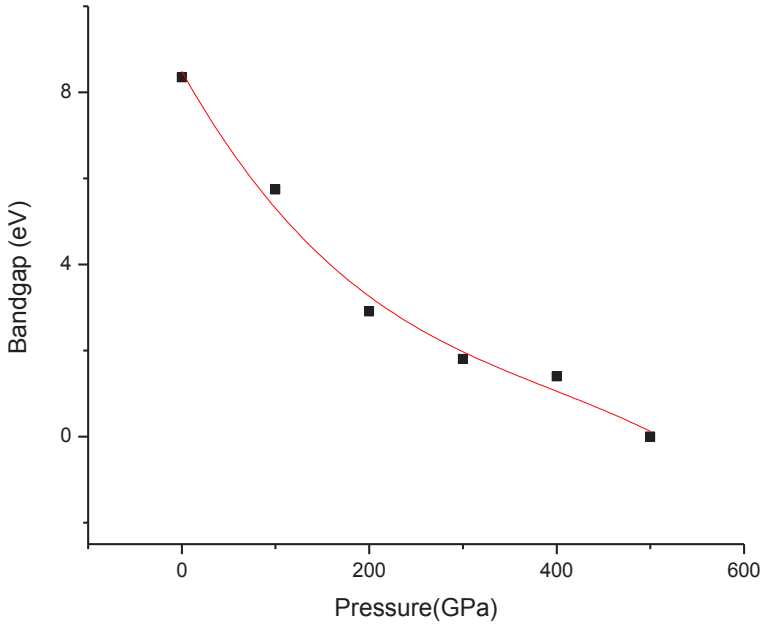
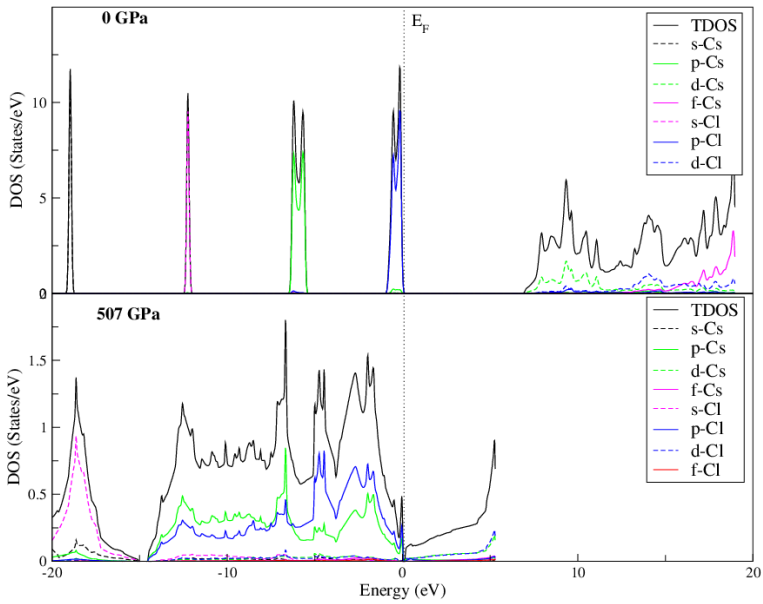Fig. 4.   Band gap as function of pressure according to Eq. (1).

Fig. 5.   DOS for CsCl at 0 GPa and 507 GPa.

going down from Fermi level. Above the Fermi level, the lower part of CB is mainly composed of Cs-5d state and upper part is mixture of Cs-5d, 4f and Cl-3p states. At 507 GPa, the DOS plot for CsCl clearly shows the metallic nature of the compound because of overlapping of valence and conduction bands over Fermi level. There are four distinct bands below the Fermi level at zero pressure while at 507 GPa, only two bands are seen in the same energy range which indicates a large variation in the electronic nature of the compound under high pressure. Valence band is dominantly occupied by mixed Cl-3p and Cs-5p states, while above the Fermi level, Cl-3d and Cs-5d states contribute majorly in CB.

3.3. *Optical properties*

In this section, we report the frequency dependent optical properties like dielectric function, reflectivity, refractive index, optical conductivity of CsCl at different pressures ranging from 0 GPa to 507 GPa with a step of 100 GPa. Optical properties are band gap dependant. As the calculated band gap is under estimated by 1.4 eV, therefore optical properties at this band gap will also be under estimated. To overcome this and predict the correct optical spectra, we have used scissor operator of 1.4 eV.

The response of a material to the incident photons is completely described by the real and imaginary parts of the dielectric function. Imaginary part of the dielectric function, $\varepsilon_2(\omega)$, provides the absorptive behavior of compounds. The variation in the $\varepsilon_2(\omega)$ with pressure is depicted in Fig. 6. At zero pressure, the absorption edge
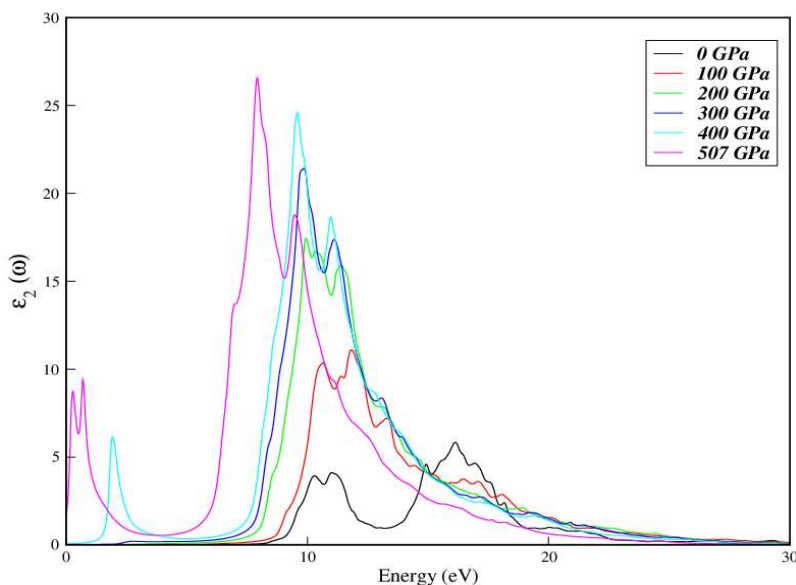

Fig. 6. The imaginary part of dielectric function for CsCl from 0 GPa to 507 GPa.

comes at 8.347 eV which is in correspondence to the band gap of the material. This first threshold is because of the transition of electrons from top of the valence band to bottom of the CB at Γ symmetry point. With the increase of pressure, the absorption edge shifts towards lower energy and at 507 GPa it has large value at 0 eV which indicates the metallic nature of the compound. Hence, CsCl becomes metal at pressure of 507 GPa. At zero pressure, peaks are observed at 8.9 eV and 9.81 eV. Other small peaks are also observed between 13 eV and 16.5 eV. The peaks at 8.9 eV and 9.81 eV are due to the transition of electrons from Cl-3p state of valence band to the Cs-5d state of CB. The multipeaks in the range 13–16.5 eV are due to the interband transitions of electrons from Cl-3p and Cs-5d states of valence band to the unoccupied Cl-3d, Cs-5d and Cs-4f states of the CB. Beyond these high peaks, small peaks are originated because of transition of electrons from bands lower than the valence band to the Cl-3d, Cs-5d and Cs-4f states of the CB. On increase in pressure one can note that these peaks are shifted towards the lower energy. This shift in energy suggests decrease in band gap which is in agreement to the electronic band structure. Also the absorption behavior of the compound changes from multipeaks to single peak which is due to the broadening of the valence band as seen from Fig. 5.

The real part of dielectric function, $\varepsilon_1(\omega)$, at various pressure ranging from 0 GPa to 507 GPa is also depicted in Fig. 7. The zero frequency limit (static) $\varepsilon_1(0)$ is 2.64 at zero pressure which is in close agreement to the experimental value of 2.67 (Ref. 28) and improved over theoretical value 3.16.[16] When the pressure
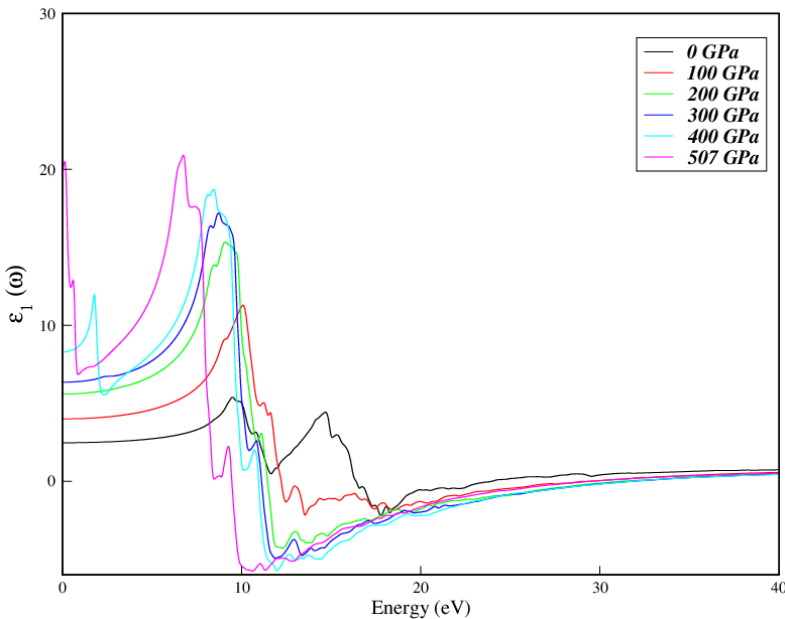

Fig. 7.   The real part of dielectric function for CsCl from 0 GPa to 507 GPa.
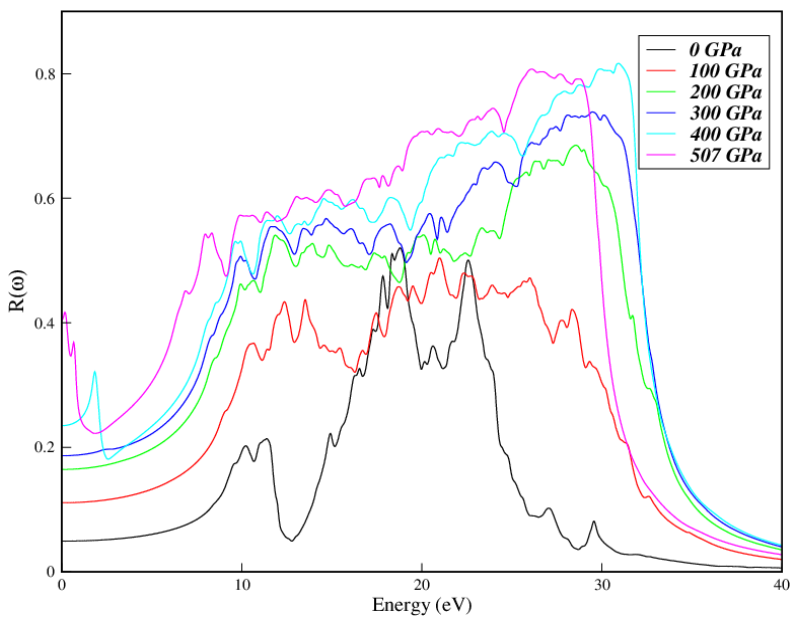
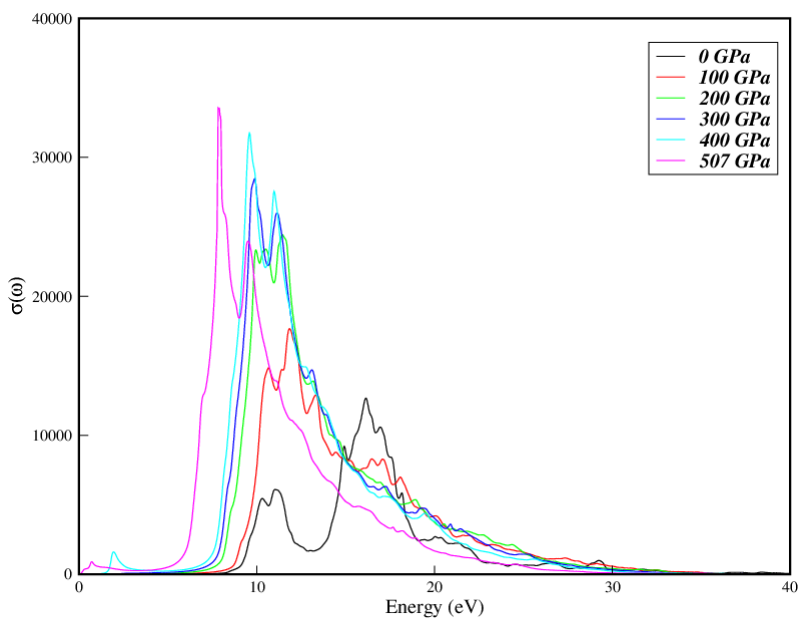Fig. 8.   The reflectivity for CsCl from 0 GPa to 507 GPa.

Fig. 9.   The optical conductivity for CsCl from 0 GPa to 507 GPa.

increases, the $\varepsilon_1(0)$ increases and its value is 21 at 507 GPa. As the band gap decreases with the increase of pressure for CsCl and $\varepsilon_1(0)$ increases with the increase of pressure therefore $\varepsilon_1(0)$ has inverse relation with the band gap. The inverse relation of $\varepsilon_1(0)$ with band gap has also been seen for other materials.[25,26] It is further seen from the spectrum that beyond the zero frequency limit, $\varepsilon_1(\omega)$ increases and become maximum at particular frequency. At 507 GPa, the spectrum of $\varepsilon_1(\omega)$ resembles the typical optical spectrum of metals[27] i.e., high value of $\varepsilon_1(\omega)$ at zero frequency and then it sharply decreases, instead of increasing. Beyond the peak value, $\varepsilon_1(\omega)$ decreases and with few variations it goes below zero and become negative in the range 16.39–23.98 eV, 12.23–29.42 eV, 11.46–31.22 eV, 11.14–31.8 eV, 10.97–31.85 eV, 9.45–29.6 eV, for 0, 100, 200, 300, 400 and 507 GPa respectively. In these energy ranges light completely attenuated. Moreover, our calculated zero frequency refractive index $n = 1.63$, also, has close agreement to the experimental one of 1.64.[29]

The reflectivity of the CsCl at various pressures is shown in Fig. 8. Zero frequency reflectivity, $R(0)$, at 0 GPa is 7% and it increases with the increase in pressure and at 507 GPa it is 41%. High peaks are shifted towards higher energies and maximum reflectivity at zero pressure is 50% which increases with pressure up to 78% at 507 GPa. At zero frequency, the reflectivity is maximum in the range 14–22 eV with multipeaks at various energy. With the increase in pressure, the maximum reflectivity range enhances. As the reflectivity is maximum when $\varepsilon_1(\omega)$ is below zero,[25] therefore the maximum reflectivity range of the compound under pressure enhances in accordance to the negative value of $\varepsilon_1(\omega)$.

In Fig. 9, we depicted the optical conductivity of CsCl for various pressures. At 0 GPa, optical conductivity starts from 8.35 eV and with the increase in pressure up to 507 GPa, the threshold point shifted towards lower energy and conduction starts at 0 eV which indicate the metallicity of the compound. After the threshold point optical conductivity increases and becomes maximum with values 12,616.7, 17,673.2, 24,434.3, 28,254, 31,729.4 and 33,568 Ω^{-1} cm^{-1} at 0, 100, 200, 300, 400 and 507 GPa, respectively. Due to the broadening of valence band, the multipeaks behavior changes to single peak. Also, due to the decrease in band gap with the increase in pressure the maximum conductivity peak shifted towards lower energies.

4. Conclusions

The calculations have been performed using FP-LAPW method with the GGA and mBJ potentials to obtain the structural and optoelectronic properties of the CsCl under high pressure. The lattice constant and band gap of the compound decrease with the increase in pressure. CsCl transforms from insulator to metal at 507 GPa. With the increase in pressure, the peaks of real and imaginary parts of dielectric function and optical conductivity shifted towards lower energy, while peaks of reflectivity shifted towards higher energy.

Acknowledgments

References

1. A. K. Brewer, *Pharmacol. Biochem. Behav.* **21**, 11 (1984).
2. H. E. Sartori, *Pharmacol. Biochem. Behav.* **21**, 11 (1984).
3. J. C. Low *et al.*, *Int. J. Dev. Neurosci.* **60**, 821 (2007).
4. J. R. Carrea *et al.*, *Am. Heart J. B* **68**, 627 (1964).
5. McGeehan and T. John, *J. Am. Med. Assoc.* **204**, 585 (1968).
6. M. P. Kowalski *et al.*, *Appl. Opt.* **25**, 2440 (1986).
7. K. M. Wong, *Jpn. J. Appl. Phys.* **48**, 085002 (2009).
8. P. Avakian and A. Smakula, *Phys. Rev.* **120**, 2007 (1960).
9. J. Visscher and R. M. Kellogg, *J. Am. Chem. Soc.* **107**, 3981 (1985).
10. H. Ehrenreich and D. Turnbull, *Solid State Physics*, Vol. 38 (Academic Press, New York, 1984), p. 29.
11. A. Lushchik *et al.*, *J. Phys. Condens. Matter.* **6**, 2357 (1994).
12. G. Yoshikawa *et al.*, *Surf. Sci.* **544**, 220 (2003).
13. S. Tsuchiya, M. Green and R. R. A. Syms, *Electrochem. Soild-State Lett.* **3**, 44 (2000).
14. N. C. Pyper, *J. Chem. Phys.* **118**, 2308 (2003).
15. J. J. Max and C. Chapados, *J. Chem. Phys.* **113**, 6803 (2000).
16. M. B. Nardelli, S. Baroni and P. Giannozzi, *Phys. Rev. B* **51**, 8060 (1995).
17. R. Reichline *et al.*, *Phys. Rev. Lett.* **56**, 2858 (1986).
18. M. I. Eremets *et al.*, *Science* **281**, 1333 (1998).
19. Y. K. Vohra *et al.*, *Phys. Rev. Lett.* **55**, 977 (1985).
20. K. M. Wong *et al.*, *J. Appl. Phys.* **113**, 014304 (2013).
21. K. M. Wong *et al.*, *J. Appl. Phys.* **114**, 034901 (2013).
22. P. Blaha *et al.*, WIEN2K, *An Augmented Plane Wave Plus Local Orbitals Program for Calculating Crystal Properties*, (Vienna University of Technology, Austria, 2001).
23. Z. Wu and R. E. Cohen, *Phys. Rev. B* **73**, 235116 (2006).
24. F. Tran and P. Blaha, *Phys. Rev. Lett.* **102**, 226401 (2009).
25. A. Sajid, G. Murtaza and A. H. Reshak, *Mod. Phys. Lett. B* **27**, 1350061 (2013).
26. G. Murtaza and I. Ahmad, *J. Appl. Phys.* **111**, 123116 (2012).
27. C. Ambrosch-Draxl and J. O. Sofo, *Comput. Phys. Commun.* **175**, 1 (2006).
28. R. P. Lowndes and D. H. Martin, *Proc. R. Soc. London* **308**, 473 (1969).
29. J. Bass, *Handbook of Optics*, 2nd edn. Vol. 2 (McGraw-Hill, 1994).
30. R. W. G. Wyckoff, *Crystal Structures* (R. E. Krieger Publishing Company, Malabar, 1982), Chap. III.
31. R. K. Singh, H. N. Gupta and M. K. Agrawal, *Phys. Rev. B* **17**, 894 (1978).